Tianjin Daxue Xuebao (Ziran Kexue yu Gongcheng Jishu Ban)/
Journal of Tianjin University Science and Technology
ISSN (Online): 0493-2137
E-Publication: Online Open Access
Vol:54 Issue:12:2021
DOI 10.17605/OSF.IO/A6GR9

RESPONSE SURFACE ANALYSIS AND OPTIMIZATION OF LASER PARAMETERS FOR MINIMUM WEAR RATE IN TUNGSTEN CARBIDE HARDFACED SURFACES

S.VIMALRAJ[1]*, Dr. R. VARAHAMOORTHI[1] and Dr. C. SUNDARRAJ[2]

[1]Department of Manufacturing Engineering, Annamalai University, Tamil Nadu, India.
[2]AVC College of Engineering, Mannampandal, Mayiladuthurai
*Corresponding Author Email: vimalbcet@gmail.com

ABSTRACT:

Process parameters are critical for laser hardfacing quality; nevertheless, these values are typicallyfound by trial and error, which incurs significant time and human expenses. In this study, the parameters of hardfaced surfaces were optimized to reduce the wear rate of tungsten carbide (WC) hardfaced on 316 L stainless steel (SS). The result of procedure parameters on wear rate is addressedin order to get the best possible condition. The trials were carried out by a response Surface methodology (RSM) based central composite design (CCD) with five levels and four factors. RSM was used to create the empirical relationship. The interplay effects of laser hardfaced surface input process factors on Wear Rate are addressed. The influencing parameter and the optimal process parameter for wear rate are identified. The laser power of 2.51 kW, travel speed 1066.96 mm/min,defocusing distance 50.00 mm, and powder feed rate 25.76 g/min were determined in this study toreach the minimal wear rate of 0.0062 mg. The provided parameter settings are shown to be beneficial in our results.

Key words: *Optimization, RSM, Tungsten Carbide, Laser Hardfacing, AISI 316L SS.*

1. INTRODUCTION:

Surface modification is a useful technique for achieving significant modifications on the material surfaces. Coating is a process that involves depositing various materials on a surface to increase qualities such as wear resistance, roughness and hardness (1) when compared to other materials, stainless steel (SS) 316L has a high density, less cost and widely available material. The percentage of Nickel content of SS 316L which makes resistant to wear and corrosion (2,3). The biocompatibility of the SS 316L would be negatively affected if nickel was released due to friction (2). A chromium oxide film protects the surface from the SS 316L wear environment. As a result, improving wear resistance and preventing nickel release are critical (4). Wear occurs when material is removed from a component, reducing its performance and lifespan. It is a sort of failure caused by surface contact; as a result, modification of substrate surface is necessary to enhance the wear resistance and enable the components to work better (5). The use of appropriate wear resistant materials (6,7) for the deposition of hardfacing layers on the parts can help to increase machine component wear resistance. In this regard, tungsten carbides WC are frequently utilized in the hard phase with combinations of nickel or cobalt-based

Tianjin Daxue Xuebao (Ziran Kexue yu Gongcheng Jishu Ban)/
Journal of Tianjin University Science and Technology
ISSN (Online): 0493-2137
E-Publication: Online Open Access
Vol:54 Issue:12:2021
DOI 10.17605/OSF.IO/A6GR9

alloys. Tungsten carbides are commonly sold as alloy powders made up of blinding WC particles with a hardness of 1500–2000 HV (8). Response Surface Methodology (RSM) was used to improve the wear results; this method involves employing modeling approaches to determine the link between the independent and dependent variables for an experiment. For designing and optimizing process variables, RSM is a combination of statistical and mathematical model tools (9). RSM has develop a regular procedure in engineering challenges, and it has been widely used in the characterization of situations in which input factors have an impact on some output variables. RSM gives quantitative measures of potential factor interactions that are hard to achieve with other optimization techniques. Using RSM, the process parameters was optimized by Huiping et al. (10). RSM is the best method for dealing with answers that are influenced by multiple variables. The number of experiments necessary to respond to a model is greatly reduced using this strategy (11). There has only been a little amount of research done on the wear behavior of tungsten carbide deposited surfaces. The wear test on tungsten carbide deposited on SS 316L was carried out under various process conditions and optimized using RSM in this research.

2. EXPERIMENTAL WORK:

2.1. Materials

The substrate material used in this research was austenitic stainless-steel SS 316L, and its composition in Wt% is reported in Table 1. The thickness of the substrate is 14 mm, with a length of 100 mm and a width of 800 mm. Stainless steel 316 L is an austenitic chromium-nickel alloy. Tungsten carbide (WC) is a chemical compound, that contains carbon and tungsten atoms in equalamounts.

Table 1: Austenitic SS 316L chemical composition in wt.%

C	Cr	Ni	Mo	Mn	P	S	Si	Fe
0.03	16.5-18.5	10.0-13.0	2.0-2.5	2.00	0.045	0.03	1.00	Balance

2.2. Laser hardfacing process

A single layer of material was applied to the substrate during the experiments. A diode laser used in this study. The highest peak power of this equipment is 4 kW. The process is influenced by a number of variables, including Travel Speed (T), Powder Feed Rate (F), Laser Power (P), and Defocusing Distance (D). Important factors such as travel speed, powder feed rate, laser power, and defocusing distance were chosen because the purpose of this study is to reduce wear. Table 2 shows the parameter levels that were chosen for this study. The experiment was carried out using center composite design to alter the parameters. The main reason of fracture formation is the modification in thermal expansion coefficients between the hardfacing powder and the substrate material. The specimen was warmed using a heater, and the surface preheating

Tianjin Daxue Xuebao (Ziran Kexue yu Gongcheng Jishu Ban)/
Journal of Tianjin University Science and Technology
ISSN (Online): 0493-2137
E-Publication: Online Open Access
Vol:54 Issue:12:2021
DOI 10.17605/OSF.IO/A6GR9

temperature was measured with a thermometer. The scanner was used to visualize the bead profile and geometries at high resolution. Microstructural characterization and composition were investigated using a Scanning Electron Microscope (SEM) attached with Energy Dispersive Spectroscopy (EDS). The wear rate of the deposits was determined using an ASTM G105 Slurry abrasion test apparatus set up at room temperature. Electro-discharge machining was used to extricate specimens from the hardfaced SS plate. On the wear test specimens, polishing was done. The specimen weight after each wear test was used to measure wear resistance. The specimen was adequately cleaned in methanol and dried in air before and after the wear test. The weight loss was precisely measured at0.0001 mg.

Table 2: Laser hardfacing parameters and their limits.

Parameters	**Units**	**Notations**	**Levels**				
			-2	**-1**	**0**	**1**	**2**
Laser Power	kW	P	2.1	2.3	2.5	2.7	2.9
Travel Speed	mm/min	T	600	800	1000	1200	1400
Defocusing Distance	mm	D	20	30	40	50	60
Powder Feed Rate	g/min	F	15	20	25	30	35

2.3 Experimental design matrix:

The design matrix was chosen as the center composite rotatable factorial design with 30 set of experiments. The center point is formed by combining all intermediate level variables with the other intermediate level variables at a lower (- 2) or higher (+2) value, whereas the star points are formed by combining all intermediate level variables with the other intermediate level variables at a lower (-2) or higher (+2) value. As a result, the 30 experimental runs shown in Table 3 were created.

Table 3: Experimental Design Matrix and its actual values.

	Coded Value				**Actual Value**				**Response**
S.No	**P (kW)**	**T (mm/ min)**	**D (mm)**	**F (g/min)**	**P (kW)**	**T (mm/min)**	**D (mm)**	**F (g/min)**	**Wear Rate(mg)**
1	-1	-1	-1	-1	2.3	800	30	20	0.0100
2	1	-1	-1	-1	2.7	800	30	20	0.0092
3	-1	1	-1	-1	2.3	1200	30	20	0.0097
4	1	1	-1	-1	2.7	1200	30	20	0.0083
5	-1	-1	1	-1	2.3	800	50	20	0.0090
6	1	-1	1	-1	2.7	800	50	20	0.0088

Tianjin Daxue Xuebao (Ziran Kexue yu Gongcheng Jishu Ban)/
Journal of Tianjin University Science and Technology
ISSN (Online): 0493-2137
E-Publication: Online Open Access
Vol:54 Issue:12:2021
DOI 10.17605/OSF.IO/A6GR9

7	-1	1	1	-1	2.3	1200	50	20	0.0080
8	1	1	1	-1	2.7	1200	50	20	0.0076
9	-1	-1	-1	1	2.3	800	30	30	0.0080
10	1	-1	-1	1	2.7	800	30	30	0.0077
11	-1	1	-1	1	2.3	1200	30	30	0.0082
12	1	1	-1	1	2.7	1200	30	30	0.0076
13	-1	-1	1	1	2.3	800	50	30	0.0079
14	1	-1	1	1	2.7	800	50	30	0.0079
15	-1	1	1	1	2.3	1200	50	30	0.0077
16	1	1	1	1	2.7	1200	50	30	0.0076
17	-2	0	0	0	2.1	1000	40	25	0.0096
18	2	0	0	0	2.9	1000	40	25	0.0091
19	0	-2	0	0	2.5	600	40	25	0.0091
20	0	2	0	0	2.5	1400	40	25	0.0080
21	0	0	-2	0	2.5	1000	20	25	0.0073
22	0	0	2	0	2.5	1000	60	25	0.0063
23	0	0	0	-2	2.5	1000	40	15	0.0097
24	0	0	0	2	2.5	1000	40	35	0.0082
25	0	0	0	0	2.5	1000	40	25	0.0062
26	0	0	0	0	2.5	1000	40	25	0.0066
27	0	0	0	0	2.5	1000	40	25	0.0066
28	0	0	0	0	2.5	1000	40	25	0.0067
29	0	0	0	0	2.5	1000	40	25	0.0067
30	0	0	0	0	2.5	1000	40	25	0.0065

Figure. 1. SEM image of uncoated SS 316 L material.

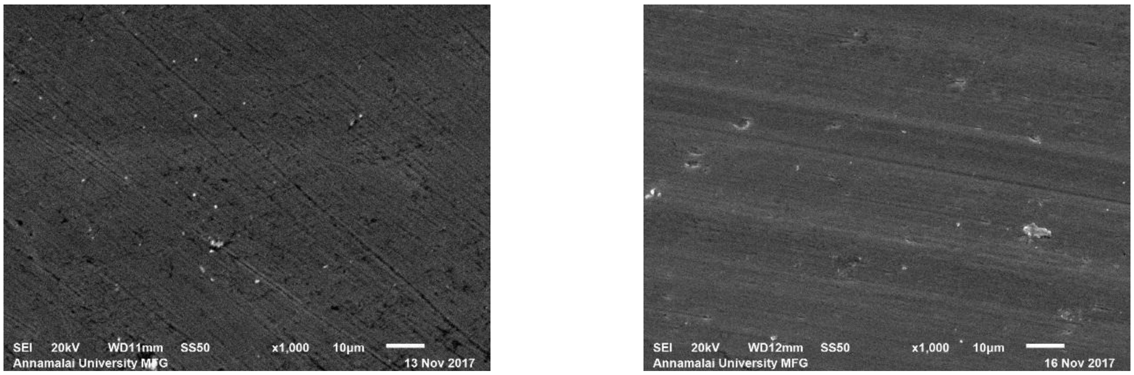

Tianjin Daxue Xuebao (Ziran Kexue yu Gongcheng Jishu Ban)/
Journal of Tianjin University Science and Technology
ISSN (Online): 0493-2137
E-Publication: Online Open Access
Vol:54 Issue:12:2021
DOI 10.17605/OSF.IO/A6GR9

Figure. 2. SEM image of coated SS 316 L material using Tungsten carbide.

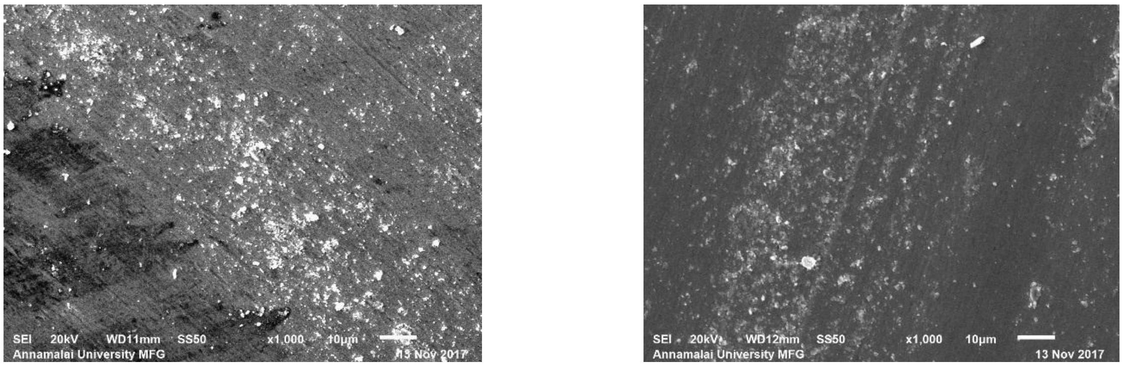

Figure 1 depicts the 316L surface morphology, while Figure 2 depicts the SEM morphology of the WC coated steel surface that shows molten (WC) globules called macro droplets released at high sliding velocity and dropped on the base material's surface as white and spherical spots. Incident macro droplets induce inhomogeneity on the WC coated surface. In Fig.2, spherical-shaped particles and nickel-chromiun irregular blocks can be seen, as well as tungsten carbide powders with carbide grains primarily composed of nickel-cobalt binded tungsten carbide particle agglomerates.

3. MODELLING:

The response surface methodology (RSM) connects dependent and independent variables to explore their interactions and establish a suitable relationship between them, in order to predict andoptimize the wear rate. Literature was used to identify important elements that determine the specific wear rate. Laser hardfaced surface wear rate is a function of laser parameters such as P, D.T and F, which can be written as

Wear Rate of Laser Hardfaced surfaces = f (P, T, D, F)
The response surface Y is predicted using a second-order polynomial equation, which is given by

The chosen polynomial might be stated identically for four factors.

$$\text{Wear Rate} = b_0 + b_a(P) + b_b(T) + b_c(D) + b_d(F) + b_{ab}(PT) + b_{ac}(PD) + b_{ad}(PF) + b_{bc}(TD) + b_{bd}(TF) + b_{cd}(DF) + b_{aa}(P^2) + b_{bb}(T^2) + b_{cc}(D^2) + b_{dd}(F^2)$$

Tianjin Daxue Xuebao (Ziran Kexue yu Gongcheng Jishu Ban)/
Journal of Tianjin University Science and Technology
ISSN (Online): 0493-2137
E-Publication: Online Open Access
Vol:54 Issue:12:2021
DOI 10.17605/OSF.IO/A6GR9

where, b_0 is the mean value of the response and b_a, b_b, b_c…b_d are linear, interactions and square terms of factors. The model and the model terms are found to be significant based on F-value (80.12) and "Prob > F" less than 0.0500 respectively. If the model terms have values greater than 0.1000, they are not significant. Model reduction may progress the model if there are many inconsequential model terms (except those essential to support hierarchy). In comparison to the pure error, the "Lack of Fit F-value" of 0.81 suggests that the Lack of Fit is insignificant. There is a 63.55% chance that a "Lack of Fit F-value" this large could occur due to noise. Non-significant lack of fit is good, we need the model to fit. At a 95% confidence level, the value of the co-efficientwas evaluated using Design Expert software. Table.4 lists the t-test and p values that were used to determine the significance of each co-efficient. Only these coefficients were used to create the final empirical connection, and developed model to predict the wear rate is shown below.

Wear Rate = +0.16504 - 0.090615 * (P) - 2.35208E-005 * (T) - 3.07917E-004 * (D) - 1.90125E-003 * (F) - 1.87500E-006 * (P) * (T) + 7.50000E – 005 * (P) * (D) + 1.12500E-004 * (P) * (F) - 5.00000E-008 * (T) * (D) +1.87500E-007 * (T)* (F) +4.25000E-006* (D) * (F) +0.017135 * (P)2+1.21354E-008*(T)2+4.79167E-007*(D)2+2.34167E-005(F)2

Tianjin Daxue Xuebao (Ziran Kexue yu Gongcheng Jishu Ban)/
Journal of Tianjin University Science and Technology
ISSN (Online): 0493-2137
E-Publication: Online Open Access
Vol:54 Issue:12:2021
DOI 10.17605/OSF.IO/A6GR9

Table 4: Anova results

Source	Sum of Squares	df	Mean Square	F Value	p-value Prob > F	Remarks
Model	3.440E-005	14	2.457E-006	80.12	< 0.0001	significant
P	9.600E-007	1	9.600E-007	31.30	< 0.0001	
T	1.500E-006	1	1.500E-006	48.91	< 0.0001	
D	1.602E-006	1	1.602E-006	52.23	< 0.0001	
F	5.042E-006	1	5.042E-006	164.40	< 0.0001	
PT	9.000E-008	1	9.000E-008	2.93	0.1073	
PD	3.600E-007	1	3.600E-007	11.74	0.0038	
PF	2.025E-007	1	2.025E-007	6.60	0.0213	
TD	1.600E-007	1	1.600E-007	5.22	0.0373	
TF	5.625E-007	1	5.625E-007	18.34	0.0007	
DF	7.225E-007	1	7.225E-007	23.56	0.0002	
P^2	1.289E-005	1	1.289E-005	420.19	< 0.0001	
T^2	6.463E-006	1	6.463E-006	210.75	< 0.0001	
D^2	6.298E-008	1	6.298E-008	2.05	0.1724	
F^2	9.400E-006	1	9.400E-006	306.53	< 0.0001	
Residual	4.600E-007	15	3.067E-008			
Lack of Fit	2.850E-007	10	2.850E-008	0.81	0.6355	not significant
Pure Error	1.750E-007	5	3.500E-008			
Cor Total	3.486E-005	29				
R^2	0.9868		Std. Dev.	1.751E-004		
Adj R^2	0.9745		Mean	7.993E-003		
Pred R^2	0.9457		C.V. %	2.19		
Adeq Precision	30.553		PRESS	1.894E-006		

3.1 Predicted Values and Actual Values:

Figure3: Correlation Graph.

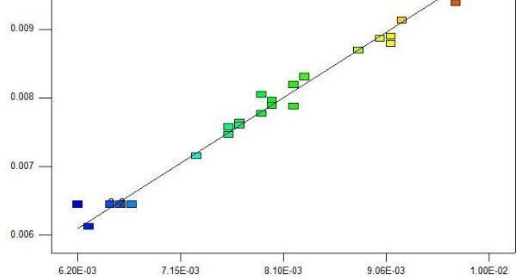

Tianjin Daxue Xuebao (Ziran Kexue yu Gongcheng Jishu Ban)/
Journal of Tianjin University Science and Technology
ISSN (Online): 0493-2137
E-Publication: Online Open Access
Vol:54 Issue:12:2021
DOI 10.17605/OSF.IO/A6GR9

Figure 4: Perturbation Graph.

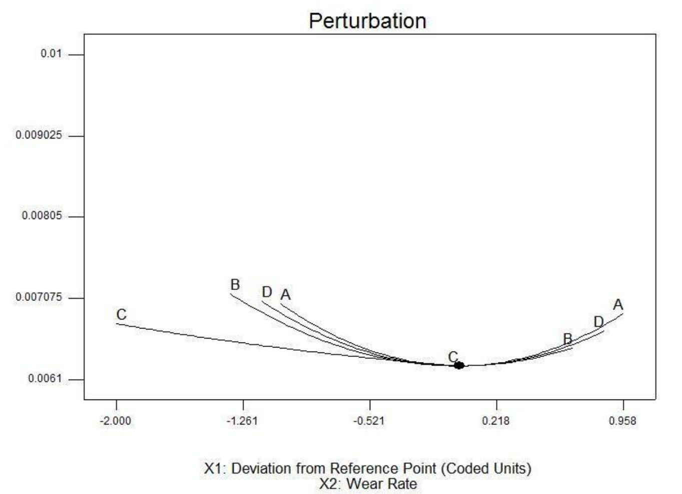

4. RESULTS AND DISCUSSION:

Dilutions (substrate melted area to total hardfacing area ratio) rise as laser power (P) rises and decrease when deposited powder amount increases, which is in agreement with the previous studies on coaxial laser hardfacing [12]. Powder deposition effectiveness is the net quantity of deposited powder that is efficiently fused to the substrate. With increasing Laser Power, Powder Feed Rate, and Travel Speed, this efficiency increases. The process features behave similarly in this situation, with the exception of a decrease in overall powder efficiency, that could be attributed to the higher amount of laser power required to heat and bind a larger number of carbide particlesinto the metallic matrix.

Figure.4 illustrates the response of the laser hardfaced surface's Wear Rate to disturbance. Every laser hardfacing parameter transfers from the reference point while all other parameters are held constant as the orientation value. This graph shows the change of Wear Rate, as well as an outline perspective of the response. By default, the design of experiment places the reference point in thecenter of the design space. It can be seen from the Figure 4 and Figure (5A-5F) that the Wear Rate lowers as the Powder Feed Rate increases. Due to the increased hardness of the laser hardfaced surface, it may be validated. With increased laser power, the rate of wear increases. The increased heat input is intended to increase penetration depth and dilution. The contour plot plays an important part in the understanding of the response surface. It becomes more colorful as the Wear Rate falls as the Powder feeding Rate and defocusing distance increase. With increased laser powerand travel speed, the wear rate increases.

Tianjin Daxue Xuebao (Ziran Kexue yu Gongcheng Jishu Ban)/
Journal of Tianjin University Science and Technology
ISSN (Online): 0493-2137
E-Publication: Online Open Access
Vol:54 Issue:12:2021
DOI 10.17605/OSF.IO/A6GR9

4.1 The Response surface and contour plots:

Figure 5A: Contour and surface showing interaction between travel speed and laser power.

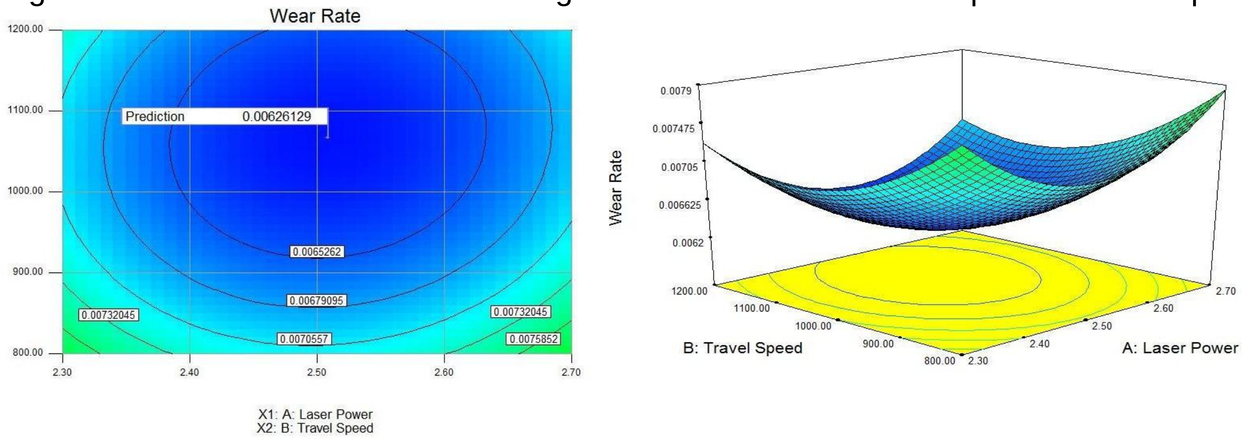

Figure 5B: Contour and surface showing interaction between laser power and defocusing distance.

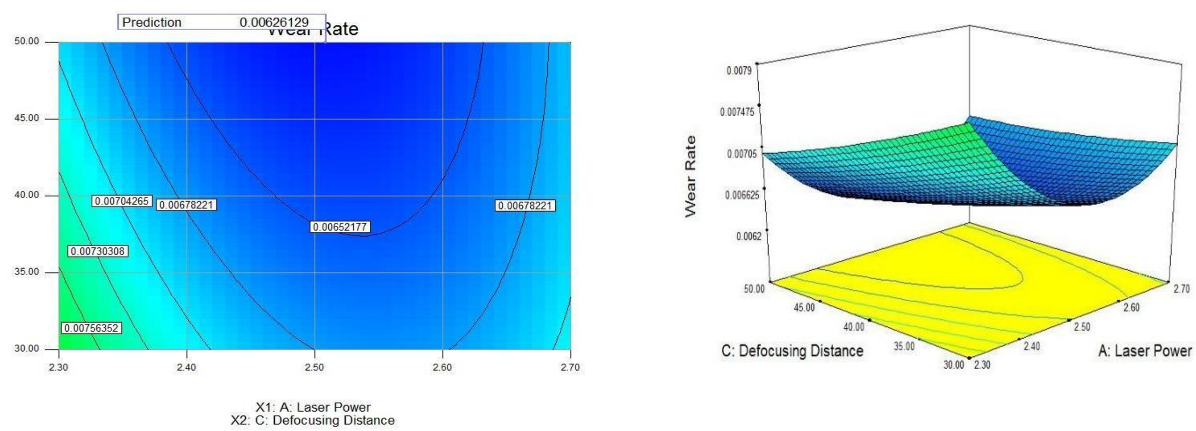

Figure 5C: Contour and surface showing interaction between powder feed rate and laser power

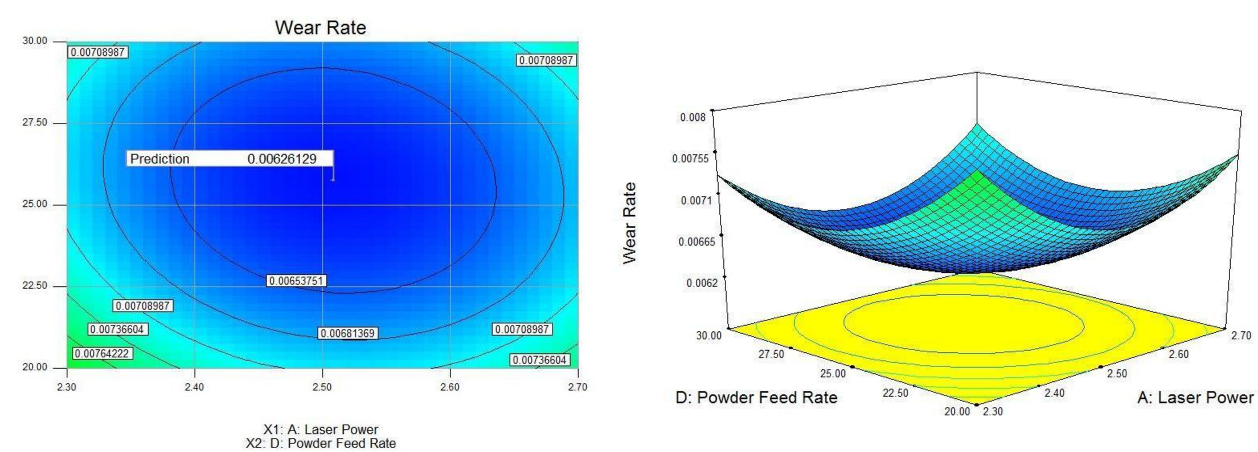

Tianjin Daxue Xuebao (Ziran Kexue yu Gongcheng Jishu Ban)/
Journal of Tianjin University Science and Technology
ISSN (Online): 0493-2137
E-Publication: Online Open Access
Vol:54 Issue:12:2021
DOI 10.17605/OSF.IO/A6GR9

Figure 5D: Contour and surface showing interaction between travel speed and defocusing distance.

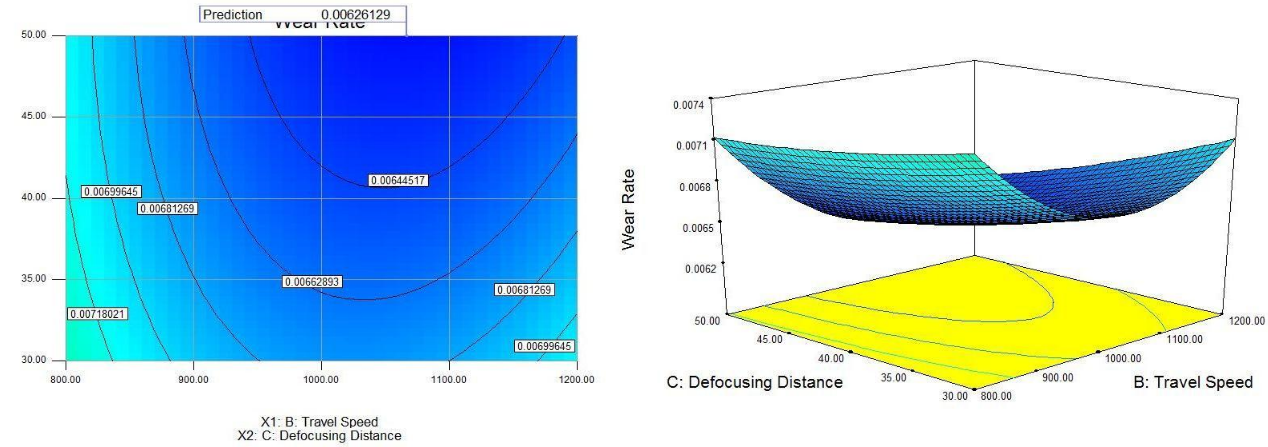

Figure 5E: Contour and surface showing interaction between powder feed rate and travel speed.

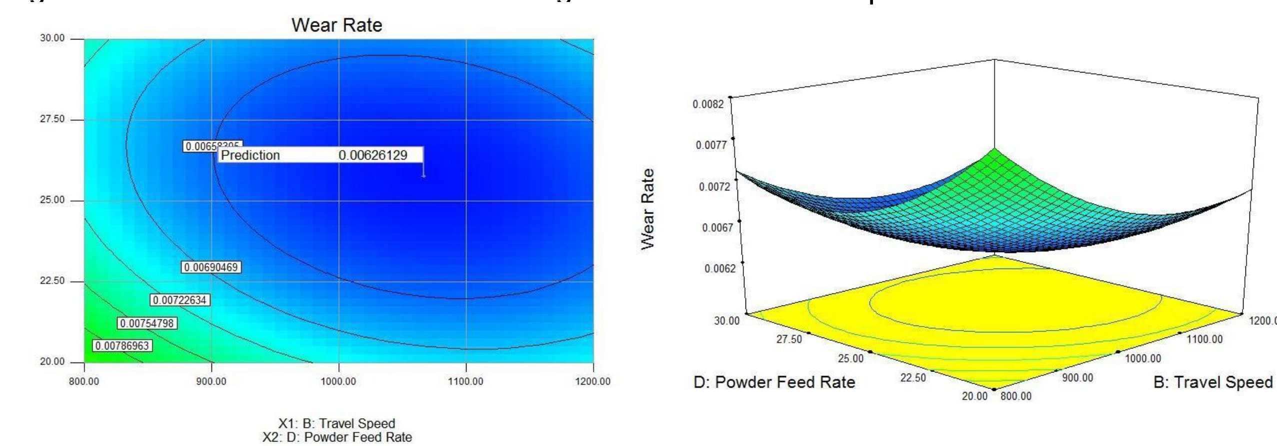

Figure 5F: Contour and surface showing interaction between powder feedrate and defocusing distance

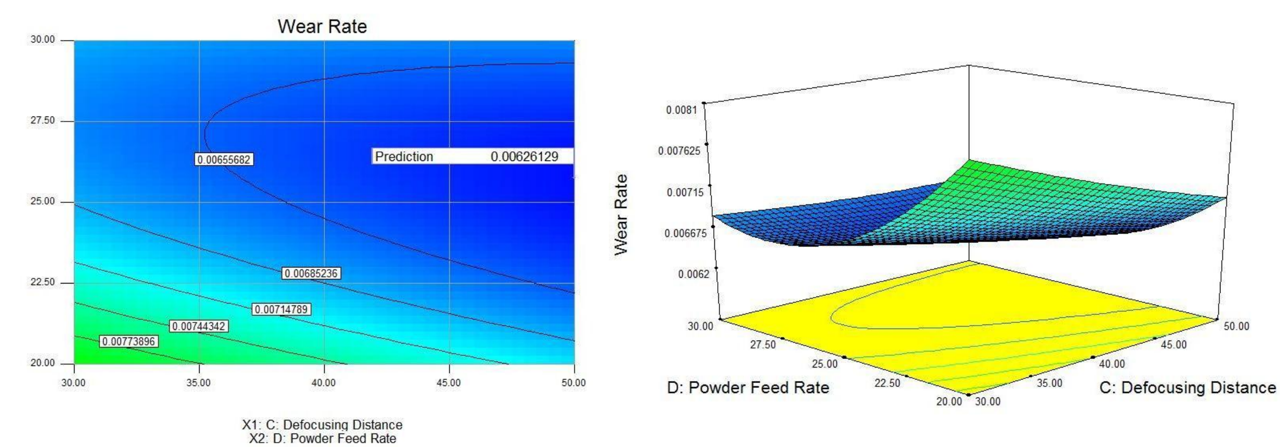

Figure 5 (A–F), it is evident that, the wear rate reduces when the powder feeding rate and defocusing distance increases The wear rate drops to a minimum while process parameters like

Tianjin Daxue Xuebao (Ziran Kexue yu Gongcheng Jishu Ban)/
Journal of Tianjin University Science and Technology
ISSN (Online): 0493-2137
E-Publication: Online Open Access
Vol:54 Issue:12:2021
DOI 10.17605/OSF.IO/A6GR9

travel speed and laser power were increased, and then it starts to multiply. Dilution, hardness, and microstructure all influence wear rate. Because the hardfacing powder material is melted with more heat, However, to melt the substrate material, only a minimum quantity of heat is necessary, the dilution rate reduces when the powder feed rate is raised. As a result, the Wear Rate begins todecrease. The rate of dilution lowers as the defocusing distance increases, leading in a reduction inwear rate to some extent. The powder density per square area decreases as the transfer speed increases, resulting in an increase in the dilution rate and a rise in the wear rate value. Laser poweris primarily utilized to melt powder, however as it increases, a large volume of substrate materialmelts, resulting in an increase in dilution, as the fluctuation in wear rate in laser hardfaced samples can be influenced by dilution. The hardness of the laser hardfaced sample decreases as a result ofincreased dilution, resulting in an increase in wear rate. As a result, the dilution should be reducedto a bare minimum in order to achieve the lowest possible wear rate. The dilution rate increases when the laser power is increased, and the Wear Rate is multiplied. The optimal rounded values of laser hardfacing parameters are presented in Table.5 after studying the response surface and contour plots. From the response surface and contour plots, it is discovered that the P of 2.51 (kW), T of 1066.96 (mm/min), D of 50.00 (mm), and F of 25.76 (g/min) can reach a minimum wear rateof 0.0062 (mg).

Figure 6: Numerical Solutions Ramps Plot.

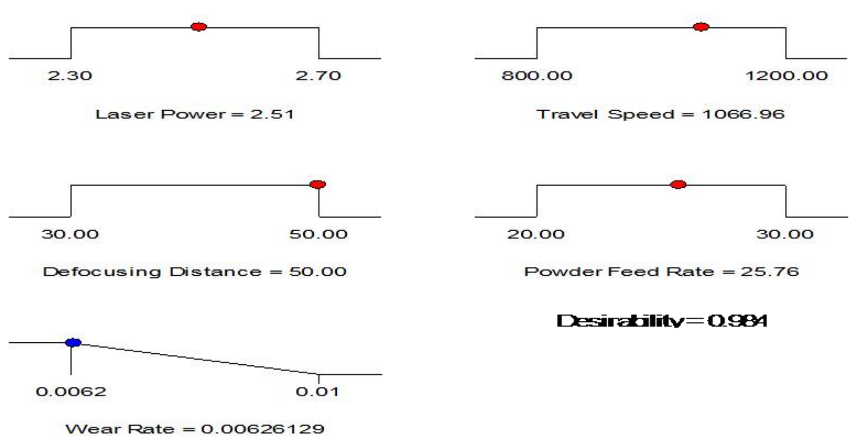

Table 5: Optimized Laser Hardfacing Parameters.

S. No	Laser Parameters	Optimized Value
1	Laser Power	2.51
2	Travel Speed	1066.96
3	Defocusing Distance	50.00
4	Powder Feed Rate	25.76

Tianjin Daxue Xuebao (Ziran Kexue yu Gongcheng Jishu Ban)/
Journal of Tianjin University Science and Technology
ISSN (Online): 0493-2137
E-Publication: Online Open Access
Vol:54 Issue:12:2021
DOI 10.17605/OSF.IO/A6GR9

5. CONCLUSIONS:

1. Under optimal hardfacing conditions, AISI 316L stainless steel plates were successfully hardfaced by laser without defects.

2. A model was developed to predict the wear rate in WC hardfaced layers fabricated on AISI 316LSS substrate with a 95% confidence level.

3. A minimum Wear Rate of 0.0062(mg) could be achieved in the Laser hardfaced surface whichwas produced by the P of 2.51(kW), T of 1066.96 (mm/min), D of 50 (mm) and F of 25.76 (g/min).

4. The Powder Feed Rate is identified as the major influencing factor than other three laser hardfacing parameters to evaluate the wear rate of hardfaced surfaces.

REFERENCES

[1] Abad MD, Munoz-Marquez M, El Mrabet S, Justo A, Sanchez-Lopez JC. Tailored synthesis of nanostructured WC/a-C coatings by dual magnetron sputtering. Surf Coat Techno 2010;204(21–22):3490–500.

[2] Guemmaz M, Moser A, Grob JJ, Stuck R. Sub-surface modification induced by nitrogen ion implantation in stainless steel (SS316L), Correlation microstructure and Nano indentation results. Surf Coat Techno 1998;100–101:353–7.

[3] Wei P, Lein S, Chin S, Jinn S. Boron- a doped Si grown by ultra-high vacuum chemical vapordeposition. Mater Chem Phys 2002; 77:426–9.

[4] Liu Chenglong, Lin Guoqiang, Yang Dazhi, Qi Min. In vitro corrosion behavior of multilayered Ti/TiN coating on biomedical AISI 316L stainless steel. Surf Coat Techno 2006; 200:4011–6.

[5] Dearnley PA, Aldrich-Smith G. Corrosion–wear mechanisms of hard coated austenitic 316L stainless steels. Wear 2004;256(5):491–9.

[6] J.E. Ferna´ ndez, P. Vijande, R. Tucho, J. Rodrı´guez, A. Martı´n, Wear 250 (2001) 11–18.

[7] Olson, D.L., Cross C.E., Friction and wear in the mining and mineral industries, ASTM Handbook, vol. 18, ASM International. Materials Park, OH, USA (1992) pp.649–655.

[8] M.J. Tobar, C. Alvarez, J.M. Amado, G. Rodrı´guez, A. Ya´n˜ez, Surf. Coat. Technol. 200 (2006) 6313–6317.

[9] Oraon B, Majumdar G, Ghosh B. Parametric optimization and prediction of electroless Ni–B deposition. Mater Des 2007; 28:2138–47.

[10] Huiping L, Guoqun Z, Shanting N, Yiguo L. Technologic parameter optimization of gas quenching process using response surface methods. Comput Mater Sci 2007; 38:561–70.

[11] Velmanirajan K, Syed Abu Thaheer A, Narayanasamy R, Ahamed Basha C. Numerical modelling of aluminum sheets formability using response surface methodology. Mater Des 2012;41:239–54.

[12] U. de Oliveira, V. Ocelik, J.Th.M. De Hosson, Surf. Coat. Technol. 197 (2005) 127–136.